Tuning the Properties of Transparent Oxide Conductors. Dopant Ion Size and Electronic Structure Effects on CdO-Based Transparent Conducting Oxides. Ga- and In-Doped CdO Thin Films Grown by MOCVD

Shu Jin,[†,‡] Yu Yang,[†,‡] Julia E. Medvedeva,[§,⊥] Lian Wang,[†,‡] Shuyou Li,[†,‡] Norma Cortes,[‡,#] John R. Ireland,[#] Andrew W. Metz,[†,‡] Jun Ni,[†,‡] Mark C. Hersam,[*,‡,#] Arthur J. Freeman,[*,§] and Tobin J. Marks[*,†,‡]

Department of Chemistry, Materials Research Center, Department of Physics and Astronomy, and Department of Materials Science and Engineering, Northwestern University, Evanston, Illinois 60208-3113, and Department of Physics, University of Missouri—Rolla, Rolla, Missouri 65409

Received September 11, 2007. Revised Manuscript Received October 25, 2007

A combined experimental and theoretical/band structure investigation is reported of Ga-doped CdO (CGO) and In-doped CdO (CIO) thin films grown on both amorphous glass and single-crystal MgO(100) substrates at 410 °C by metal–organic chemical vapor deposition (MOCVD). Film phase structure, microstructure, and electrical and optical properties are systematically investigated as a function of doping stoichiometry and growth conditions. XRD data reveal that all as-deposited CGO and CIO thin films are phase-pure and polycrystalline, with features assignable to a cubic CdO-type crystal structure. Epitaxial films grown on single-crystal MgO(100) exhibit biaxial, highly textured microstructures. These as-deposited CGO and CIO thin films exhibit excellent optical transparency, with an average transmittance of >80% in the visible range. Ga and In doping widens the optical band gap from 2.85 to 3.08 and 3.18 eV, respectively, via a Burstein–Moss shift. On MgO(100), room temperature thin film conductivities of 11 500 and 20 000 S/cm are obtained at an optimum Ga and In doping levels of 1.6% and 2.6%, respectively. Together, the experimental and theoretical results reveal that dopant ionic radius and electronic configuration have a significant influence on the CdO-based TCO structural, electronic, and optical properties: (1) lattice parameters contract as a function of dopant ionic radius in the order Y (1.09 Å) < In (0.94 Å) < Sc (0.89 Å), Ga (0.76 Å), with the smallest radius ion among the four dopants only shrinking the lattice marginally and exhibiting low doping efficiency; (2) carrier mobilities and doping efficiencies decrease in the order In > Y > Sc > Ga; (3) the Sc and Y dopant d states have substantial influence on the position and width of the s-based conduction band, which ultimately determines the intrinsic charge transport characteristics.

Introduction

Transparent conducting oxides (TCOs) have gained significant attention over the past two decades, serving as key components in optoelectronic devices such as flat panel displays (FPDs), organic light-emitting diodes (OLEDs), photovoltaics, solar cells, optical waveguides, and energy-efficient windows.[1–13] Currently, tin-doped indium oxide (ITO), with a typical electrical conductivity of (3–5) × 10^3 S/cm and 85–90% transparency in the visible region, is employed on a huge scale as a transparent electrode in many display technologies. However, there are several important limitations that cloud its future applicability: (1) limited availability and high cost of indium, (2) relatively low conductivity (not suitable for large-area displays), (3) significant optical absorption in the blue-green region (not suitable for many full-color displays), and (4) chemical instability in certain device structures (e.g., corrosion in OLEDs). In view of these issues, intense research has focused on understanding fundamental TCO crystal structure–film microstructure–electronic structure–charge transport–optical transparency

* To whom correspondence should be addressed.
† Department of Chemistry, Northwestern University.
‡ Materials Research Center, Northwestern University.
§ Department of Physics and Astronomy, Northwestern University.
# Department of Materials Science and Engineering, Northwestern University.
⊥ Current address: University of Missouri—Rolla.

(1) Coutts, T. J.; Mason, T. O.; Perkins, J. D.; Ginley, D. S. *Proc. Electrochem. Soc.* **1999**, *99-11*, 274.
(2) Coutts, T. J.; Young, D. L.; Li, X. *MRS Symp. Proc.* **2000**, *623*, 199.
(3) Freeman, A. J.; Poeppelmeier, K. R.; Mason, T. O.; Chang, R. P. H.; Marks, T. J. *MRS Bull.* **2000**, *25*, 45.
(4) Ginley, D. S.; Bright, C. *MRS Bull.* **2000**, *25*, 15.
(5) Gordon, R. G. *MRS Bull.* **2000**, *25*, 52.
(6) Granqvist, C. G.; Hultaker, A. *Thin Solid Films* **2002**, *411*, 1.
(7) Hosono, H.; Ohta, H.; Orita, M.; Ueda, K.; Hirano, M. *Vacuum* **2002**, *66*, 419.
(8) Kawamura, K.; Takahashi, M.; Yagihara, M.; Nakayama, T. European Patent Application, EP1271561, A2 20030102, CAN 138:81680, AN 2003:4983, 2003.
(9) Kawazoe, H.; Yanagi, H.; Ueda, K.; Hosono, H. *MRS Bull.* **2000**, *25*, 28.
(10) Lewis, B. G.; Paine, D. C. *MRS Bull.* **2000**, *25*, 22.
(11) Mason, T. O.; Gonzalez, G. B.; Kammler, D. R.; Mansourian-Hadavi, N.; Ingram, B. J. *Thin Solid Films* **2002**, *411*, 106.
(12) Minami, T. *MRS Bull.* **2000**, *25*, 38.
(13) Wu, X.; Dhere, R. G.; Albin, D. S.; Gessert, T. A.; DeHart, C.; Keane, J. C.; Duda, A.; Coutts, T. J.; Asher, S.; Levi, D. H.; Moutinho, H. R.; Yan, Y.; Moriarty, T.; Johnston, S.; Emery, K.; Sheldon, P. *Proc. NCPV Prog. Rev. Meet., Lakewood, CO* **2001**, 47.

10.1021/cm702588m CCC: $40.75
Published on Web 12/12/2007

relationships and on searching for ITO alternatives that are less expensive and possess comparable or higher conductivity and/or wider optical transparency windows.[3,5,9,10,12,14–20]

Recently, CdO-based TCOs have received much attention due to their exceptional carrier mobilities, nearly metallic conductivities, and relatively simple crystal structures.[11,21–28] Sn doping of CdO thin films grown epitaxially on MgO(111) by pulsed laser deposition (PLD) achieves thin film mobilities and conductivities as high as 607 $cm^2/(V\ s)$ and 42 000 S/cm, respectively, rendering them the most conductive TCO thin films with the highest carrier mobilities reported to date.[26] Although the optical band gap of pure bulk CdO is only 2.3 eV,[29] leading to relatively poor optical transparency in the short wavelength range, aliovalent metal doping offers the possibility of tuning the electronic structure and the optical band gap through a carrier concentration-dependent Burstein–Moss (B–M) energy level shift.[30,31] CdO, with a simple cubic rock salt structure, broadly dispersed s-like conduction band, and a small carrier effective mass, is considered to be an ideal model material in which to study the effects of doping on TCO band structure, crystal chemistry, and charge transport.

Various deposition techniques, such as reactive evaporation,[32,33] solution growth,[34] spray pyrolysis,[35,36] sputtering,[37–40] PLD,[26] and MOCVD,[23,25,27,28,41–44] have been employed to grow CdO and CdO-based thin films. For device fabrication, chemical vapor deposition offers many attractive features, such as in situ growth under a variety of atmospheres, low-cost equipment, amenability to large area coverage with high throughput, conformal coverage, easy control of growth chemistry, and the possibility of creating metastable phases.[45]

In previous work from this laboratory, undoped and doped CdO thin films were successfully grown by MOCVD using optimized metal–organic Cd precursors.[23,25,27,44] In-doped CdO thin films grown on glass by MOCVD exhibit conductivities as high as 16 800 S/cm. It was found that In-doping dramatically alters the CdO band structure by extensive mixing of In 5s and Cd 5s states, also yielding a hybridization gap in the conduction band.[44] Sc^{3+} and Y^{3+} with six-coordinate ionic radii of 0.89 and 1.04 Å, respectively, were employed to test the dopant size effects.[23,27] Compared to In^{3+} and Sn^{4+}, the s states of Sc^{3+} and Y^{3+} are located deeper in the conduction band, resulting in a weak hybridization with the Cd 5s states. Thus, these experiments also strove to assess the role of these s states. It was found that thin film conductivities as high as 6000 and 8540 S/cm are obtained on glass substrates at 1.2% Sc and 1.2% Y doping, respectively. Compared to In-doped CdO, the Sc- and Y-doped CdO (CSO, CYO) thin films on glass exhibit lower carrier mobilities and carrier concentrations, in accord with the lower dispersion of the s-like conduction band, as revealed by first-principles FLAPW electronic band structure calculations.[23] CSO and CYO thin films on MgO(100) with a maximum conductivity of 18 100 and 17 800 S/cm are obtained at a Sc doping level of ~1.8% and a Y doping level of 1.3%, respectively, which are to date the most conductive transparent conducting oxide materials grown by MOCVD. All of these MOCVD-derived thin films exhibit good optical transparency, with an average transmittance >80% in the visible range. Sc and Y doping effectively widens the band gap from 2.7 to 3.4 eV via a Burstein–Moss band-filling shift, in agreement with our screened exchange local density approximation (sX-LDA) calculations.[23,27,46]

Our continued interest in CdO-based TCOs focuses on understanding crystal structure–charge transport relationships by further doping CdO with a wide variety of dopants which simultaneously offer (1) controlled lattice parameter excursions via varying the ionic radius and (2) varying degrees of orbital overlap between the orbitals

(14) Coutts, T. J.; Young, D. L.; Li, X.; Mulligan, W. P.; Wu, X. *J. Vac. Sci. Technol., A* **2000**, *18*, 2646.
(15) Coutts, T. J.; Young, D. L.; Li, X. N. *MRS Bull.* **2000**, *25*, 58.
(16) Edwards, D. D.; Mason, T. O.; Sinkler, W.; Marks, L. D.; Goutenoire, F.; Poeppelmeier, K. R. *J. Solid State Chem.* **1998**, *140*, 242.
(17) Ott, A. W.; Chang, R. P. H. *Mater. Chem. Phys.* **1999**, *58*, 132.
(18) Phillips, J. M.; Cava, R. J.; Thomas, G. A.; Carter, S. A.; Kwo, J.; Siegrist, T.; Krajewski, J. J.; Marshall, J. H.; Peck, W. F.; Rapkine, D. H. *Appl. Phys. Lett.* **1995**, *67*, 2246.
(19) Wang, A. C.; Dai, J. Y.; Cheng, J. Z.; Chudzik, M. P.; Marks, T. J.; Chang, R. P. H.; Kannewurf, C. R. *Appl. Phys. Lett.* **1998**, *73*, 327.
(20) Wang, R. P.; King, L. L. H.; Sleight, A. W. *J. Mater. Res.* **1996**, *11*, 1659.
(21) Asahi, R.; Wang, A.; Babcock, J. R.; Edleman, N. L.; Metz, A. W.; Lane, M. A.; Dravid, V. P.; Kannewurf, C. R.; Freeman, A. J.; Marks, T. J. *Thin Solid Films* **2002**, *411*, 101.
(22) Babcock, J. R.; Wang, A. C.; Metz, A. W.; Edleman, N. L.; Metz, M. V.; Lane, M. A.; Kannewurf, C. R.; Marks, T. J. *Chem. Vap. Deposition* **2001**, *7*, 239.
(23) Jin, S.; Yang, Y.; Medvedeva, J. E.; Ireland, J. R.; Metz, A. W.; Ni, J.; Kannewurf, C. R.; Freeman, A. J.; Marks, T. J. *J. Am. Chem. Soc.* **2004**, *126*, 13787.
(24) Kammler, D. R.; Mason, T. O.; Young, D. L.; Coutts, T. J.; Ko, D.; Poeppelmeier, K. R.; Williamson, D. L. *J. Appl. Phys.* **2001**, *90*, 5979.
(25) Metz, A. W.; Ireland, J. R.; Zheng, J. G.; Lobo, R.; Yang, Y.; Ni, J.; Stern, C. L.; Dravid, V. P.; Bontemps, N.; Kannewurf, C. R.; Poeppelmeier, K. R.; Marks, T. J. *J. Am. Chem. Soc.* **2004**, *126*, 8477.
(26) Yan, M.; Lane, M.; Kannewurf, C. R.; Chang, R. P. H. *Appl. Phys. Lett.* **2001**, *78*, 2342.
(27) Yang, Y.; Jin, S.; Medvedeva, J. E.; Ireland, J. R.; Metz, A. W.; Ni, J.; Hersam, M. C.; Freeman, A. J.; Marks, T. J. *J. Am. Chem. Soc.* **2005**, *127*, 8796.
(28) Zhao, Z. Y.; Morel, D. L.; Ferekides, C. S. *Thin Solid Films* **2002**, *413*, 203.
(29) Koffyberg, F. P. *Phys. Rev. B* **1976**, *13*, 4470.
(30) Burstein, E. *Phys. Rev.* **1954**, *93*, 632.
(31) Moss, T. S. *Proc. Phys. Soc. A* **1954**, *382*, 775.
(32) Phatak, G.; Lal, R. *Thin Solid Films* **1994**, *245*, 17.
(33) Reddy, K. T. R.; Sravani, C.; Miles, R. W. *J. Cryst. Growth* **1998**, *185*, 1031.
(34) Matsuura, N.; Johnson, D. J.; Amm, D. T. *Thin Solid Films* **1997**, *295*, 260.
(35) Murthy, L. C. S.; Rao, K. *Bull. Mater. Sci.* **1999**, *22*, 953.
(36) Vigil, O.; Vaillant, L.; Cruz, F.; Santana, G.; Morales-Acevedo, A.; Contreras-Puente, G. *Thin Solid Films* **2000**, *361*, 53.
(37) Chu, T. L.; Chu, S. S. *J. Electron. Mater.* **1990**, *19*, 1003.
(38) Gurumurugan, K.; Mangalaraj, D.; Narayandass, S. K.; Nakanishi, Y.; Hatanaka, Y. *Appl. Surf. Sci.* **1997**, *113/114*, 422.
(39) Lewin, R.; Howson, R. P.; Bishop, C. A.; Ridge, M. I. *Vacuum* **1986**, *36*, 95.
(40) Subramanyam, T. K.; Uthanna, S.; Naidu, B. S. *Phys. Scr.* **1998**, *57*, 317.
(41) Gulino, A.; Castelli, F.; Dapporto, P.; Rossi, P.; Fragala, I. *Chem. Mater.* **2002**, *14*, 704.
(42) Gulino, A.; Dapporto, P.; Rossi, P.; Fragala, I. *Chem. Mater.* **2002**, *14*, 4955.
(43) Gulino, A.; Dapporto, P.; Rossi, P.; Fragala, I. *Chem. Mater.* **2002**, *14*, 1441.
(44) Wang, A.; Babcock, J. R.; Edleman, N. L.; Metz, A. W.; Lane, M. A.; Asahi, R.; Dravid, V. P.; Kannewurf, C. R.; Freeman, A. J.; Marks, T. J. *Proc. Natl. Acad. Sci. U. S.A.* **2001**, *98*, 7113.
(45) Schulz, D. L.; Marks, T. J. In *CVD of Non-metals*; Rees, W. S., Ed.; VCH: New York; pp 39–150.
(46) Medvedeva, J. E.; Freeman, A. J. *Europhys. Lett.* **2005**, *69*, 583.

that contribute to the conduction band near the Fermi level and thus govern the transport properties. Hence, Ga^{3+}, with a much smaller ionic radius than In^{3+} (0.76 Å vs 0.94 Å) and fully occupied 3d band (unlike Sc^{3+} and Y^{3+}), represents an ideal probe ion to examine dopant radius size effects; furthermore, In^{3+}, which was previously found to be the optimum dopant for CdO thin films on an amorphous glass substrates and is theoretically predicted to be an ideal doping candidate,[27,44] has never before been grown epitaxially on single crystal substrates.

In this experimental and theoretical contribution, we report the growth of Ga- and In-doped CdO (CGO, CIO) thin films on amorphous glass and single crystal MgO(100) substrates by MOCVD. The CGO and CIO thin film phase structure, microstructure, and electrical and optical properties are investigated in detail as a function of doping level, and growth parameters and are compared with CSO and CYO thin films. These results are correlated with first-principles full-potential linear augmented plane wave (FLAPW) electronic band structure calculations within the screened-exchange local density approximation (sX-LDA) to treat both ground and excited states. It will be seen that phase-pure CGO and CIO thin films exhibit conductivities of 11 500 and 20 000 S/cm, respectively, at Ga and In doping levels of 1.6% and 2.6%, respectively. Moreover, all the as-deposited TCO thin films exhibit good visible region transparency, with an average transmittance >80%. These structural, charge transport, and optical results are completely understandable within the framework of the electronic structure calculations.

Experimental Section

MOCVD Precursors and Thin Film Growth. CdO-based thin film growth was carried out in the previously described horizontal, cold-wall MOCVD reactor.[47] The volatile metal–organic Cd precursor $Cd(hfa)_2$(*N*,*N*-DE-*N*′,*N*′-DMEDA) (**1**) (hfa = hexafluoroacetylacetonate, *N*,*N*-DE-*N*′,*N*′-DMEDA = *N*,*N*-diethyl-*N*′,*N*′-dimethylethyldnediamine) was prepared from high-purity $Cd(NO_3)_2 \cdot 4H_2O$ (99.999%, Aldrich) and was triply vacuum-sublimed.[25] $Ga(dpm)_3$ (**2**) and $In(dpm)_3$ (**3**) (dpm = dipivaloymethanate) were prepared from $Ga(NO_3) \cdot 4H_2O$ (99.999%, Alfa Aesar) and $In(NO_3)_3$ (99.999%, Alfa Aesar) by literature procedures.[48–50]

For Ga- and In-doped CdO thin film growth, the precursor reservoir temperatures/Ar carrier gas flow rates were optimized at $Cd(hfa)_2$(*N*,*N*′-DE-*N*,*N*′-DMEDA), 85 °C/15 sccm; $Ga(dpm)_3$, 92 °C/6–40 sccm; $In(dpm)_3$, 94–95 °C/5–20 sccm. The O_2 oxidizing gas was introduced upstream at 400 sccm after bubbling through distilled water. A system operating pressure of 4.0 ± 0.1 Torr and a substrate temperature of 400 °C were maintained during the thin film deposition. Corning 1737F glass and polished single-crystal MgO(100) (a = 4.216 Å) substrates were purchased from Precision Glass and Optics and MTI Corp., respectively. Both the glass and the MgO(100) substrate surfaces were cleaned with acetone prior to the film deposition and were placed side-by-side on a SiC-coated susceptor in the growth reactor for simultaneous growth experiments.

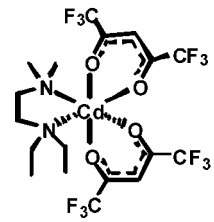

1

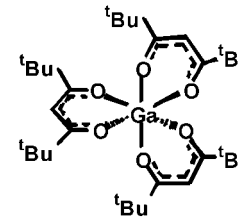

2

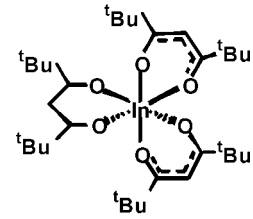

3

Thin Film Physical Characterization Measurements. Composition analyses of the present films were carried out using inductively coupled plasma atomic emission spectrometry (ICP-AES). Optical transparency measurements were carried out in the range 300–3300 nm with a Cary 500 UV–vis–NIR spectrophotometer. Film thicknesses were measured using a Tencor P-10 profilometer after etching a step in the film using 5% HCl solution. X-ray diffraction θ–2θ scans of CdO films on glass were obtained with a Rigaku DMAX-A powder diffractometer using Ni-filtered Cu Kα radiation. Rocking curves and φ scans of the epitaxial thin films on MgO(100) substrates were obtained on a home-built Rigaku four-circle diffractometer with detector-selected Cu Kα radiation. Film surface morphology was imaged using a Digital Instruments Nanoscope III atomic force microscope (AFM) operating in the contact mode. Film microstructure was imaged on a Hitachi S4500 FE scanning electron microscope (SEM). Transmission electron microscopy (TEM) images and selected area electron diffraction (SAED) patterns were obtained using a Hitachi 2000 microscope operating at 200 keV. Cross-sectional samples were prepared by mechanical grinding, dimpling, and ion milling. Ambient-temperature four-probe charge transport data were acquired on a Bio-Rad HL5500 Hall effect measurement system. Variable-temperature Hall effect and four-probe conductivity data were collected between 77 and 330 K and used instrumentation described previously.[51]

Theoretical Methods. First-principles electronic band structure calculations on 12.5 atom % Ga-doped CdO were performed using the highly precise all-electron full-potential linearized augmented plane wave (FLAPW) method[52] that has no shape approximation for the potential and charge density. The exchange-correlation potential is treated via the local density approximation (LDA). Cutoffs of the plane-wave basis (14.4 Ry) and potential representation (81.0 Ry) and expansion in terms of spherical harmonics with $l \leq 8$ inside the muffin-tin spheres were used. The equilibrium relaxed geometry of the structures was determined via total energy and atomic force minimization for the lattice parameter, a, and the internal atomic positions. Furthermore, to determine accurately the excited-state band structure of CGO, we employed the self-consistent screened-exchange local density approximation (sX-

(47) Hinds, B. J.; McNeely, R. J.; Studebaker, D. B.; Marks, T. J.; Hogan, T. P.; Schindler, J. L.; Kannewurf, C. R.; Zhang, X. F.; Miller, D. J. *J. Mater. Res.* **1997**, *12*, 1214.
(48) Jablonski, Z.; Rychlowskahimmel, I.; Dyrek, M. *Spectrochim. Acta, Part A* **1979**, *35*, 1297.
(49) Utsunomi, K *Bull. Chem. Soc. Jpn.* **1971**, *44*, 2688.
(50) Wang, A. C.; Edleman, N. L.; Babcock, J. R.; Marks, T. J.; Lane, M. A.; Brazis, P. R.; Kannewurf, C. R. *J. Mater. Res.* **2002**, *17*, 3155.
(51) Lyding, J. W.; Marcy, H. O.; Marks, T. J.; Kannewurf, C. R. *IEEE Trans. Instrum. Meas.* **1988**, *37*, 76.
(52) Cimino, A.; Marezio, M. *Phys. Chem. Solids* **1960**, *17*, 57.

LDA)[53] which is known to provide a considerably improved description of optical properties compared to the LDA. Cutoff parameters of 10.24 Ry in the wave vectors and $l \leq 3$ inside the muffin-tin spheres were used. Summations over the Brillouin zone were carried out using 10 special k points in the irreducible wedge.

Results and Discussion

We first describe CGO and CIO thin film growth by an efficient MOCVD process. Then, CGO and CIO film composition, morphology, microstructure, and epitaxy are characterized as a function of doping level using a broad array of complementary physical techniques. In addition, film optical and electrical properties are investigated and compared with those of the Sc- and Y-doped CdO analogues grown by the same technique. In doing so, we demonstrate the tunability of the CdO-based TCO materials by varying the dopants and substrates to achieve optimized transparent conductor properties. These results are compared and contrasted to those computed via first-principles band structure techniques.

Film Growth. A series of conductive CGO and CIO thin films were grown on Corning 1737F glass and single crystal MgO(100) at 410 °C and under a 400 sccm O_2 flow rate for 2 h by MOCVD. The film growth rates were ~1–2 nm/min on glass and ~1.5–2.5 nm/min on MgO(100), which are similar to those established for Sc- and Y-doped CdO. The Ga and In doping levels can be varied from 0% to 6.0% and 0% to 6.9%, respectively, by varying the Ga and In precursor reservoir temperatures and Ar carrier gas flow rates.

Film Composition, Morphology, Microstructure, and Epitaxy. X-ray diffraction $\theta-2\theta$ scans were carried out from $2\theta = 25°$ to 75°. Figure 1 shows XRD data as a function of Ga (Figure 1A) and In (Figure 1B) doping level. As can be seen from the figures, all of the films with Ga and In doping levels up to 6.0% and 6.9% are phase-pure, with a highly crystalline FCC CdO structure. No Ga_2O_3, In_2O_3, or other phases are detected by XRD, consistent with Ga^{3+} and In^{3+} substituting for the Cd^{2+} in the lattice instead of forming a new phase.

Using polycrystalline silicon as an internal calibration reference, the precise lattice parameters of the MOCVD-derived CGO and CIO thin films on glass were determined and are also compared with the results of Sc and Y doping in Figure 2. It is found that the lattice parameters are gradually compressed with increasing Ga and In doping levels. Note that with the introduction of Ga the lattice dimensions are not decreased as much as expected purely on the basis of Vegard's law dopant radius considerations, since six-coordinated Ga^{3+} with an ionic radius of 0.76 Å is far smaller than Cd^{2+} (1.09 Å). This suggests that the Ga doping efficiency is lower than for In, Sc, and Y, even though no new phase is formed. This trend is further supported by the observation that the carrier concentration increases only slightly with increased Ga doping levels (see below). In marked contrast, In^{3+}, having a six-coordinate ionic radius of 0.94 Å (more comparable to that of Cd^{2+}), compresses

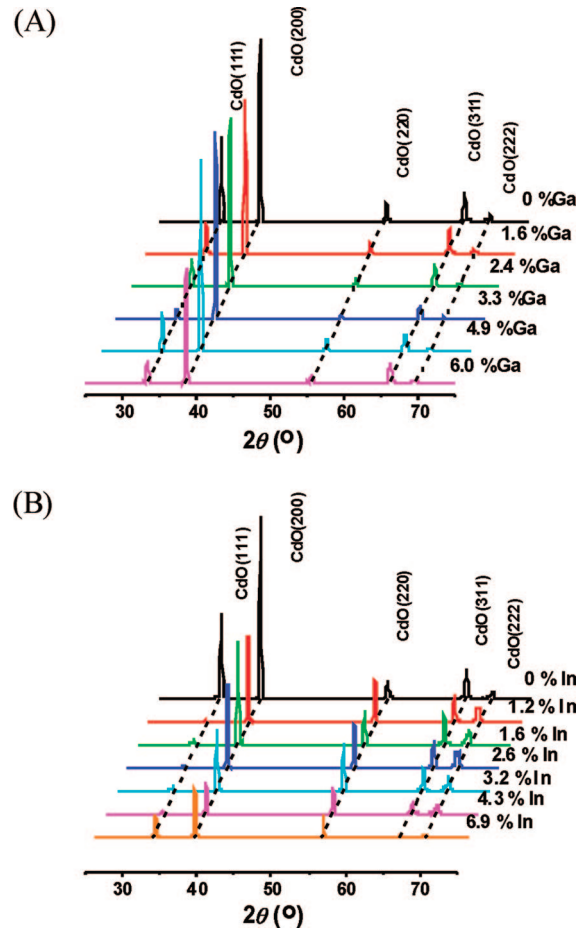

Figure 1. $\theta-2\theta$ X-ray diffractograms of CGO (A) and CIO (B) thin films grown on glass at 410 °C by MOCVD as a function of Ga and In doping level (given in atom %).

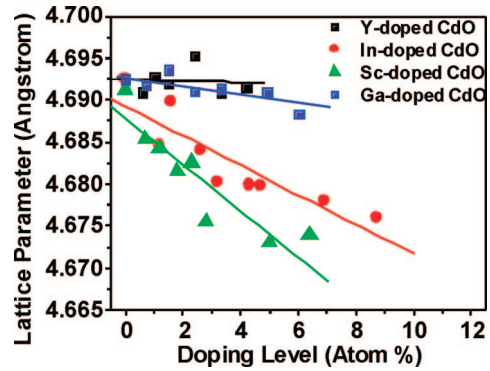

Figure 2. Lattice parameter changes as a function of dopant size and doping level for Ga-, In-, Sc-, and Y-doped CdO thin films grown on glass. Lines through the data points are drawn as a guide to the eye.

the lattice monotonically with increased doping levels, and the carrier concentration increase with In doping is consistent with a significantly greater doping efficiency. Note, however, that even the significant lattice contractions caused by progressive In doping fall below those estimated from simple Vegard's law considerations (Figure 2). This effect is likely due to compensation by the antibonding character of the conduction band formed from the Cd 5s and O 2p states as discussed previously.[23,46]

In contrast to the above results for growth on amorphous glass substrates, all CGO and CIO thin films grown on MgO(100) exhibit a highly (200) textured microstructure.

(53) Wimmer, E.; Krakauer, H.; Weinert, M.; Freeman, A. J. *Phys. Rev. B* **1981**, *24*, 864.

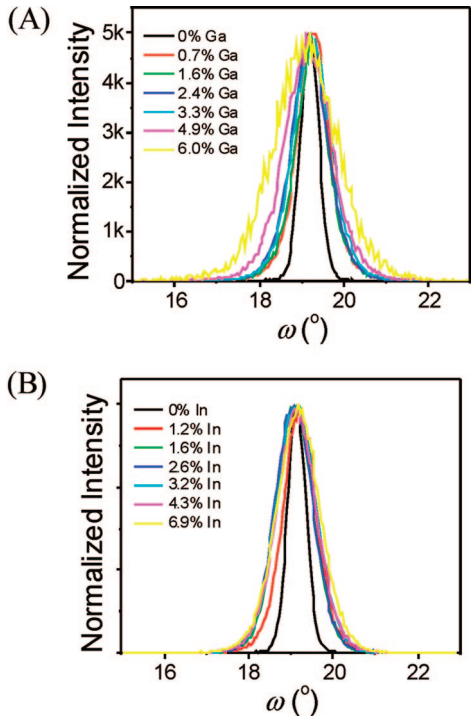

Figure 3. XRD texture analyses of CGO (A) and CIO (B) thin films grown on single-crystal MgO(100) as a function of Ga and In doping level; rocking curves measured on the CdO(200) XRD peak.

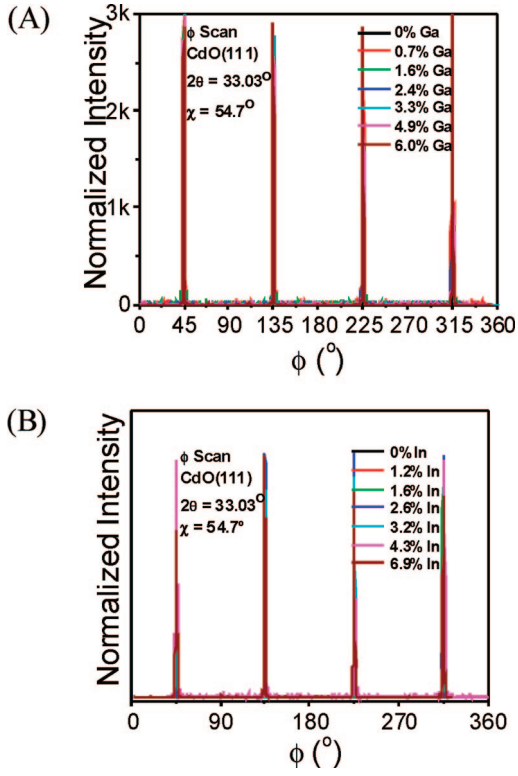

Figure 4. XRD texture analyses of CGO (A) and CIO (B) thin films grown on single-crystal MgO(100) as a function of Ga and In doping level: in-plane φ-scans measured on the CdO (111) XRD peak with $\chi = 54.7°$. Ga and In doping levels are given in atom %.

The texture of the thin films is shown in Figures 3 and 4. As can be seen from Figure 3, the rocking curves of the films show good out-of-plane alignment. The full width at half-maximum (fwhm) increases from 0.5° for pure CdO films to 1.0° and 1.0° at 2.4% Ga and 2.6% In doping,

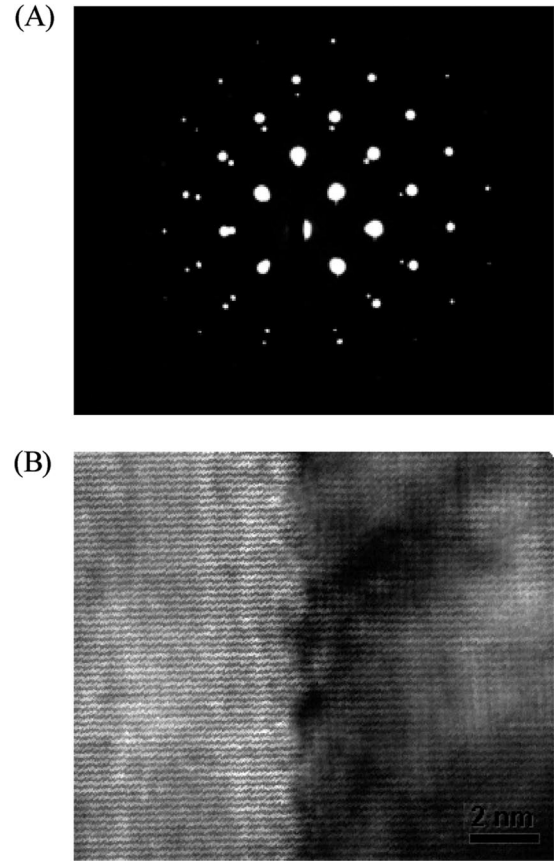

Figure 5. TEM images of 1.6% doped CGO thin film on MgO(100): (A) SAED pattern, (B) cross-section image (MgO substrate is on the left side of the image and the Ga-doped CdO film grown is on the right side).

respectively, and to 1.8° and 1.4° at 6.0% Ga and 6.9% In doping, respectively, indicating that the crystallinity decreases with increased Ga and In doping. Note that the In-doped CdO thin films have the greatest crystallinity among the four dopants studied. In-plane orientation was investigated by φ-scans of the CdO (111) reflection at $\chi = 54.7°$, and data are shown in Figure 4. The clear 4-fold rotational symmetry of the CdO (111) reflections together with the small fwhms (0.5° for pure CdO, 1.2° for CGO at 2.4% Ga doping, 1.1° for CIO at 2.6% In doping) reveal excellent in-plane orientation of the films. The orientation relations between the CGO and CIO thin films and the MgO(100) substrates are therefore CdO(100)||MgO(100).

TEM images and SAED patterns of 1.6% Ga-doped CdO films grown on MgO(100) are shown in Figure 5. The SAED pattern of the film indicates that the CdO grains retain the biaxial (in-plane and out-of-plane) texture of the single-crystal substrate. Figure 5B shows that the Ga-doped CdO thin films grow epitaxially with a highly textured crystallinity. The dark shadow on the interface of the TEM cross section indicates that most of the strain from the mismatch of the lattice ($a_{MgO} = 4.216$ Å, ~10% smaller than $a_{CdO} = 4.696$ Å) has relaxed at or near the interface.

SEM surface images in Figures 6 and 7 show that the as-deposited CGO and CIO thin films grown on glass are densely packed with heavily grained structures. At low Ga and In doping levels (≤3.2–3.3%), films on glass are all very uniform with rounded grains in plan view. With the Ga and In doping increased to 4.9% and 4.3%, respectively, and higher, the grains

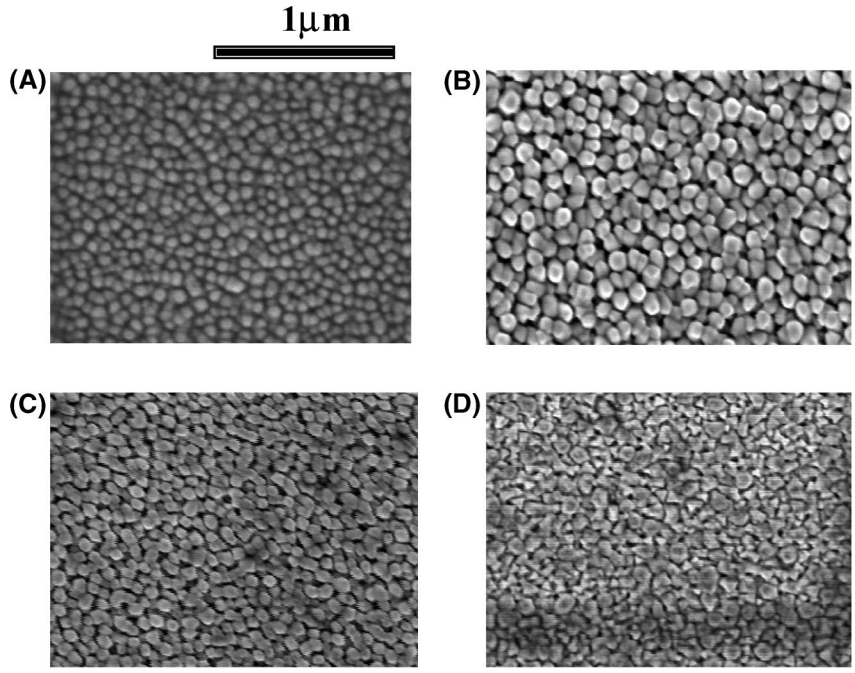

Figure 6. SEM images of CGO thin films grown on glass as a function of Ga doping level (given in atom %): (A) 0.7%, (B) 1.6%, (C) 3.3%, and (D) 4.9%.

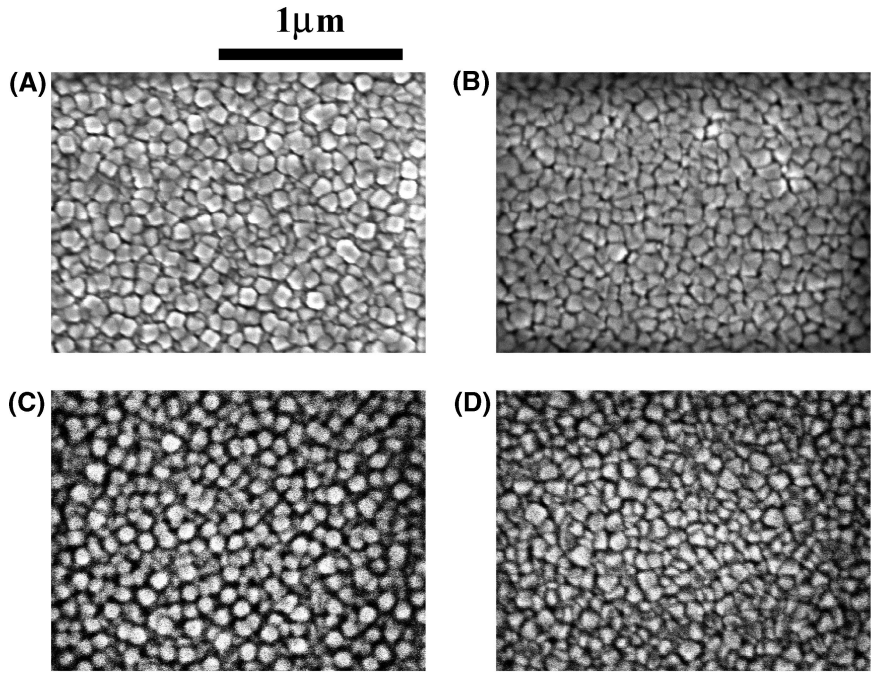

Figure 7. SEM images of CIO thin films grown on glass as a function of In doping level (given in atom %): (A) 1.2%, (B) 1.6%, (C) 3.2%, and (D) 4.3%.

of the films on glass are largely triangular in shape, suggesting that the (111) planes are parallel to the surface, which agrees well with the XRD analysis and is similar to trends observed previously in Sc and Y doping.[23,27] As for the epitaxial films on MgO(100), the films with Ga doping levels $\leq$1.6% are featureless (single-grained) by SEM and are found to be very smooth and uniform by AFM. As the Ga doping level is increased to $\geq$3.3%, a grained structure is clearly visible; the films with In doping are smoother and featureless up to 4.3% doping (single-grained) by SEM and confirmed to be very smooth and uniform by AFM. Contact-mode AFM images of the CGO and CIO thin films are shown in Figure 8. The data reveal that the CIO thin films on glass are very uniform and smooth, with root-mean-square (rms) roughnesses of 2.5–3.5 nm over a 5 μm $\times$ 5 μm area (Figure 8B), while the CGO thin films are somewhat rougher, exhibiting root-mean-square (rms) roughnesses of 7–9 nm over a 5 μm $\times$ 5 μm area (Figure 8A). Regarding the CGO and CIO films grown on MgO(100), the surface roughnesses of the films are less than those grown on glass, also similar to the Sc- and Y-doped CdO series.[23,27] The rms roughness is found to be 1–3 nm for In-doped CdO (Figure 8D) and 5–7 nm for Ga-doped Cd (Figure 8C).

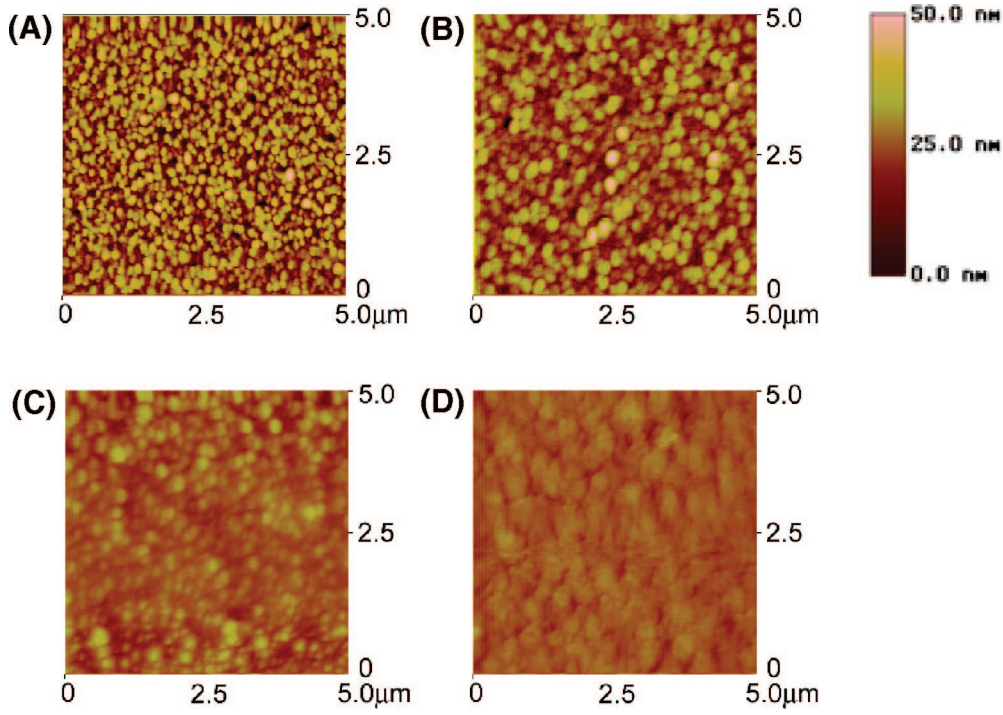

Figure 8. AFM images of CGO and CIO thin films: (A) 3.3% Ga-doped CdO on glass, rms roughness = 8.9 nm; (B) 3.3% Ga-doped CdO on MgO(100), rms roughness = 6.3 nm; (C) 3.2% In-doped CdO on glass, rms roughness = 2.5 nm; (D) 3.2% In-doped CdO MgO(100), rms roughness = 1.9 nm.

Film Optical and Electrical Properties. All of the as-grown CdO films are light-yellow to the eye but highly transparent. The color becomes lighter with increased Ga and In doping as the band edge shifts to higher energies. Optical transmission spectra of CGO and CIO thin films grown on glass are shown in Figure 9. For CGO and CIO thin films with thicknesses of ~200 nm, the average transmittance at 550 nm is ~85%. With an increase of Ga and In doping level, the band edges are found to be dramatically blue-shifted, doubtless due to the Burstein–Moss effect. Simultaneously, the plasma edges shift to the blue, owing to the increase in free carrier concentration with increased doping level. Band gap estimates were derived from the optical transmission spectra by extrapolating the linear portion of the plot of $(\alpha h\nu)^2$ vs $h\nu$ to $\alpha = 0$ (Figure 10). It is found that the band gap increases from 2.85 to 3.08 eV with an increase in Ga doping from 0% to 6.0% and to 3.18 eV with increases in In doping from 0% to 6.9%.

As in other ailovalent metal-doped CdO materials investigated to date, all of the Ga- and In-doped CdO film samples exhibit n-type conductivity as determined by negative Hall coefficients. Figure 11 shows the temperature dependence of thin film charge transport properties for a 2.7 atom % CGO film on MgO (100). Similar to Y- and Sc-doped CdO,[23,27] the mobilities and conductivities of CGO films are essentially independent of temperature in the low-temperature region (<100 K), suggesting that neutral impurity scattering (NIS) and/or ionized impurity scattering (IIS) processes are dominant.[25,54–57] In the high-temperature region (>100 K), the mobility and conductivity decrease with increasing temperature, suggesting that lattice vibration scattering (LVS), which is temperature-dependent, has now become an important scattering contributor.[58–60] The importance of grain boundary scattering (GBS) is an incompletely resolved mechanistic issue in most CdO-based TCOs. It has been argued that GBS is insignificant for highly degenerate TCOs because the carrier mean free paths (determined optically) are typically much smaller than the grain sizes of typical films.[25,54,59–62]

Electrical conductivity, mobility, and carrier concentration data for as-grown CdO thin films as a function of Ga and In doping level are plotted. Data for Y- and Sc-doped thin films are also compared in Figures 12–14. For the present In-doped CdO films, with an increase in In doping, the carrier concentration increases from 2.3×10^{20} cm^{-3} for pure CdO thin films on glass to 9.3×10^{20} cm^{-3} at ~4.3% In doping, while for the Ga-doped CdO thin films, the carrier concentration increases only marginally to 4.4×10^{20} cm^{-3} at 4.9% Ga doping. The GCO mobility, however, drops precipitously with increased Ga doping. However, in the case of In doping, due to the more effective overlap of the In and Cd 5s orbitals, the mobility falls at a far slower rate compared to the mobility in Y-, Sc-, and Ga-doped CdO. It is clear from these data that M^{3+} (M = Ga, In, Sc, and Y) ions behave as effective dopants by replacing Cd^{2+} sites in the lattice and donating electrons to act as charge carriers. However, at certain doping

(54) Asahi, R.; Mannstadt, W.; Freeman, A. J. *Phys. Rev. B* **1999**, *59*, 7486.
(55) Dingle, R. B. *Philos. Mag.* **1955**, *46*, 831.
(56) Erginsoy, C. *Phys. Rev.* **1950**, *79*, 1013.
(57) Frank, G.; Koestlin, H. *Appl. Phys. A: Mater. Sci. Process.* **1982**, *A27*, 197.
(58) Bardeen, J.; Shockley, W. *Phys. Rev.* **1950**, *80*, 72.
(59) Chen, M.; Pei, Z. L.; Wang, X.; Yu, Y. H.; Liu, X. H.; Sun, C.; Wen, L. S. *J. Phys. D: Appl. Phys.* **2000**, *33*, 2538.
(60) Zhang, D. H.; Ma, H. L. *Appl. Phys. A: Mater. Sci. Process.* **1996**, *62*, 487.
(61) Gilmore, A. S.; Al-Kaoud, A.; Kaydanov, V.; Ohno, T. R. *MRS Symp. Proc.* **2001**, *666*, 10/1.
(62) Tahar, R. B. H.; Tahar, N. B. H. *J. Appl. Phys.* **2002**, *92*, 4498.

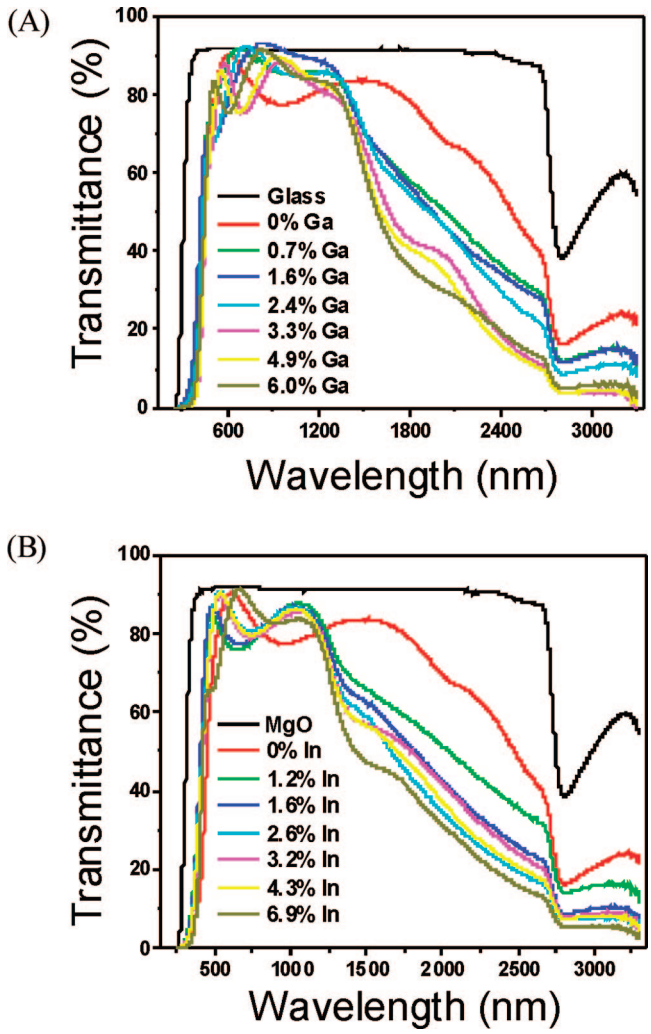

Figure 9. Transmission optical characterization of MOCVD-derived CGO (A) and CIO (B) thin films grown on glass as a function of Ga and In doping level.

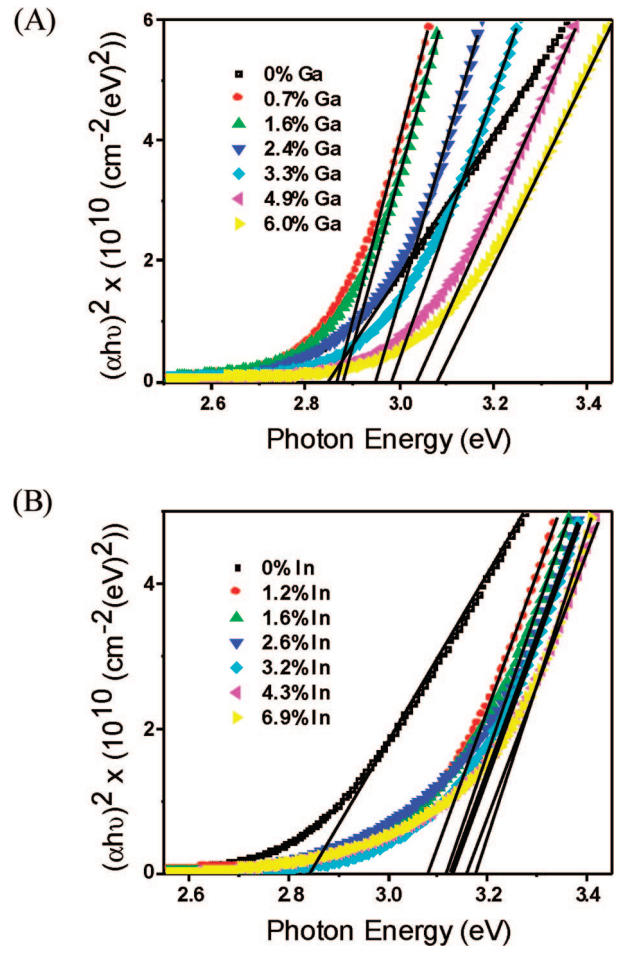

Figure 10. Transmission optical characterization of MOCVD-derived CGO (A) and CIO (B) thin films grown on glass as a function of Ga and In doping level: band gap estimates.

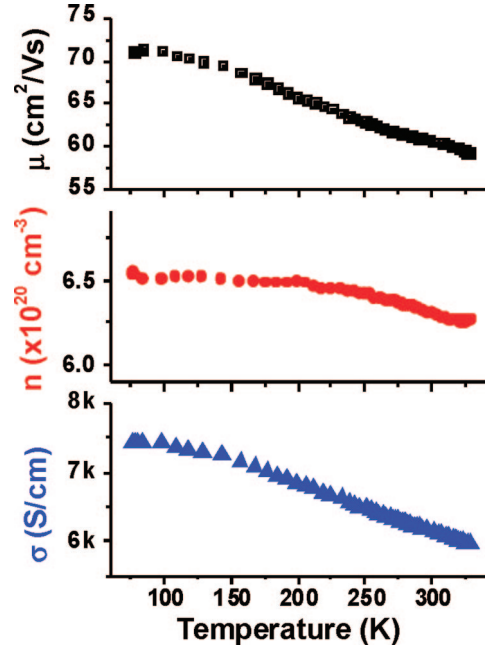

Figure 11. Variable-temperature electrical conductivity and Hall effect measurements for a 2.7 atom % Ga-doped CdO thin film on MgO(100): carrier mobility (■), carrier concentration (●), and electrical conductivity (▲).

levels (2–5%), the carrier density plateaus and the mobilities decline substantially, indicating that some of the M dopant sites may not be readily ionized and/or do not contribute to the mobile charge carriers. In addition, excess M doping appears to degrade the thin film crystallinity and increase carrier scattering, thereby decreasing carrier mobility and conductivity. Compared with In doping, much less Ga can be effectively doped into the CdO lattice. Thin films with maximum conductivities of 10 400 and 20 000 S/cm on glass and MgO(100), respectively, are obtained at 4.3% and 2.6% In doping. Compared with films on glass, CIO films on MgO(100), at the same doping level, exhibit similar doping level-dependent trends but exhibit much greater carrier concentrations and mobilities, indicating that the epitaxial films possess fewer scattering centers and higher doping efficiency due to their highly textured microstructure/enhanced crystalline perfection, similar to behavior found for epitaxial CdO on MgO(100) and epitaxial ITO on single-crystal YSZ.[63] In the contrasting case of Ga doping, which exhibits much lower doping efficiency, the conductivity of the doped thin films on glass falls with increasing Ga doping levels and essentially never achieves the pure CdO level. CGO films grown on MgO(100), with the contribution of epitaxial effects, exhibit higher doping efficiency, and a

(63) Taga, N.; Odaka, H.; Shigesato, Y.; Yasui, I.; Kamei, M.; Haynes, T. E. *J. Appl. Phys.* **1996**, *80*, 978.

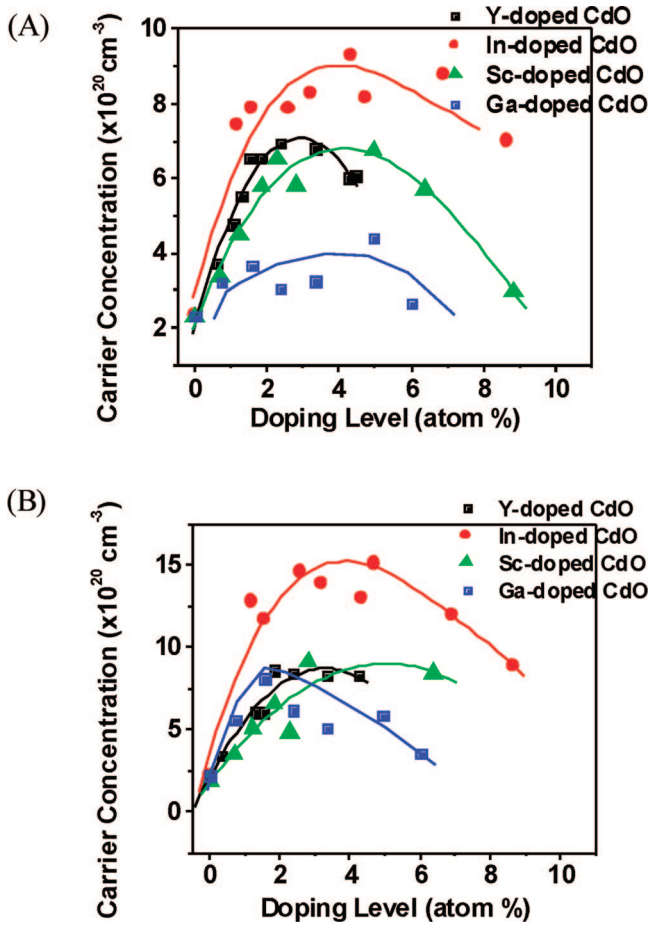

Figure 12. Room temperature four-probe charge transport measurements for Ga-, Y-, In-, and Sc-doped CdO thin films on glass (A) and on MgO(100) (B): carrier concentration. Lines are drawn as a guide to the eye.

maximum conductivity of 11 500 S/cm is achieved at a 1.6% doping level. In addition, comparison of the charge transport properties for Ga-, In-, Y-, and Sc-doped CdO given in Figures 12–14 shows that carrier mobilities and doping efficiencies decrease in the order In > Y > Sc > Ga.

Band Structure Calculations. The total energy FLAPW method[52] was used to carry out full optimization of the CGO crystal structure (both the lattice and internal parameters were optimized) at 12.5 atom % Ga doping. We find that the computed lattice parameter of CGO, $a = 4.62$ Å, is smaller than that of pure CdO (4.66 Å, as obtained from a separate total energy FLAPW calculation). This is consistent with the smaller ionic radius of Ga^{3+} (0.76 Å) as compared to that of Cd^{2+} (1.09 Å). We find that substitution with Ga results in a large structural relaxation so that the distance between Cd and its nearest O neighbors increases by 9%, from 2.33 to 2.54 Å. The distance between Ga and the oxygen ions is 2.08 Å. Comparing these findings with our previous results for CdO doped with In, Y, and Sc, it can be seen that the variation in the Cd–O distances in CdO doped with the various dopants correlates well with their ionic radii, namely, Y^{3+}(1.04 Å) < In^{3+} (0.94 Å) < Sc^{3+} (0.89 Å) < Ga^{3+} (0.76 Å). Because the Cd–O distance determines the hybridization between the Cd 5s states and O 2p states, its variation significantly affects the optical properties of the material, as described below.

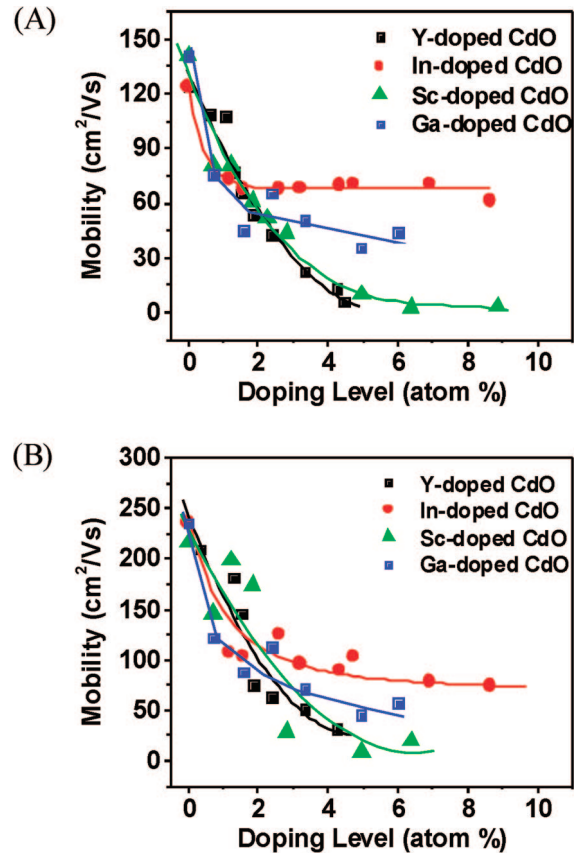

Figure 13. Room temperature four-probe charge transport measurements for Ga-, Y-, In-, and Sc-doped CdO thin films on glass (A) and on MgO(100) (B): mobility. Lines are drawn as a guide to the eye.

Figure 15 illustrates how Ga doping alters the CdO band structure and affects the optical transitions. It is seen that due to a pronounced Burstein–Moss shift, the intense interband transitions from the valence band are now significantly higher in energy. The calculated sX-LDA band gap energies which determine the optical transparency of the doped material are found to be 2.53, 3.15, and 3.39 eV in the [100], [110], and [111] directions, respectively. These values are smaller than those found for CdO doped with In, Sc, or Y at the same doping level of 12.5 atom %. We suggest that the large relaxation of the oxide anions around Ga^{3+} due to its smaller ionic radius leads to a weaker Cd 5s–O 2p hybridization, which in turn reduces the optical band gap values in the doped material. Therefore, we can conclude that a smaller dopant ion radius results in lower energy optical transitions from the valence band. We note, however, that in CGO the partially filled conduction band is split from the rest of the band by a second gap. As a result, the transitions from the Fermi level up into the conduction band are higher in energy for CGO as compared to In-, Sc-, or Y-doped CdO. These transitions contribute to the optical absorption in the visible range, although they have low intensity due to the small density of states at the Fermi level. Within the sX-LDA formalism, we find the second gaps in CGO to be 1.80, 1.62, and 0.94 eV in the [100], [110], and [111] directions, respectively, compared with those obtained for In-doped CdO, namely, 1.94, 1.54, and 0.51 eV in the [100], [110], and [111] directions, respectively. The smallest second band gap value is found

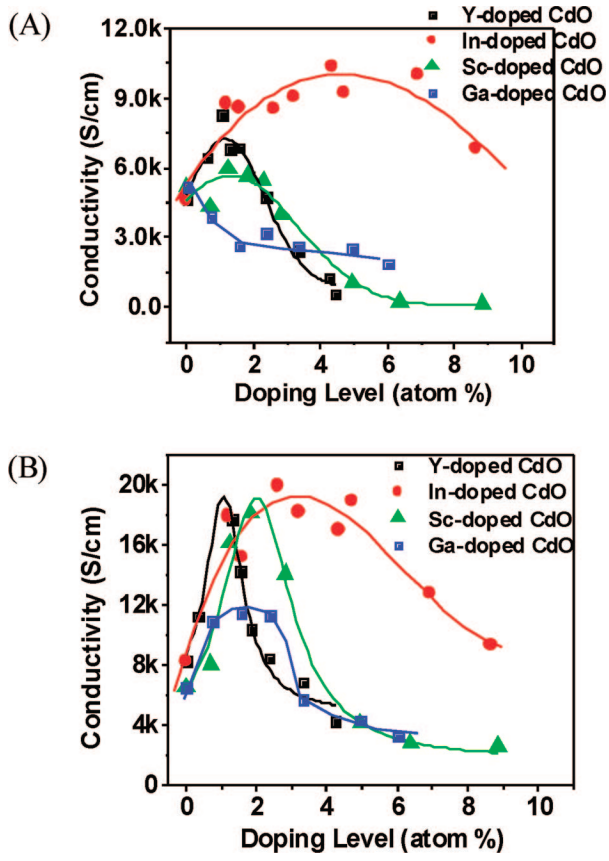

Figure 14. Room temperature four-probe charge transport measurements for Ga-, Y-, In-, and Sc-doped CdO thin films on glass (A) and on MgO(100) (B): electrical conductivity. Lines are drawn as a guide to the eye.

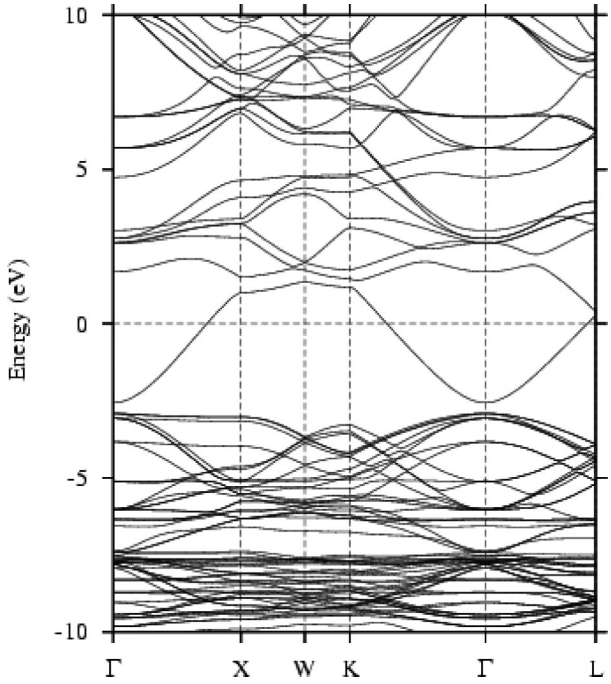

Figure 15. Calculated sX-LDA band structure for 12.5 atom % Ga-doped CdO along the high symmetry directions in the Brillouin zone.

to be in the [111] direction for all dopants investigated and is 0.51, 0.70, 0.83, and 0.94 eV for In-, Y-, Sc-, and Ga-doped CdO, respectively.

Similar to the cases of In-, Y-, and Sc-doped CdO, the highly dispersed single band crosses the Fermi level in the [100] (Δ), [110] (Λ), and [111] (Σ) directions (Figure 15). For all dopants considered, this band is formed primarily from the 5s states of Cd strongly hybridized with the p states of the oxygen atoms. We find that the contributions to the total density of states at the Fermi level from the s states of Ga (1.3%) in CGO are reduced compared to those of In (4.3%) in CIO. The calculated electron velocities at the Fermi level in CGO, found to be 0.33, 0.17, and 0.04 $\times$ 10^5 m/s in the (Δ) [100], (Λ) [110], and (Σ) [111] directions, respectively, are significantly smaller than those in In-doped CdO. These estimates of the electron velocities in Ga-, In-, Y-, and Sc-doped CdO correlate well with the width of the dispersed conduction bands, which are found to be 3.01, 3.91, 3.36, and 2.57 eV, respectively. In the case of Sc, the presence of empty d states close to the conduction band edge significantly affects the dispersion of this band, resulting in the low carrier mobility. While the d states of Ga are completely filled, the conduction band narrowing in CGO originates from the weaker Cd 5s–O 2p hybridization which appears from the large structural relaxation. Thus, our theoretical estimates agree well with the observed variation in the carrier mobility and conductivity in these systems reported above as well as in our previous work.

Conclusions

Highly conductive and transparent CGO and CIO thin films have been grown on glass and single crystal MgO(100) substrates at 410 °C by low-pressure MOCVD. As-deposited CGO and CIO thin films exhibit good optical transparency, with an average transmittance of 85% in the visible region. As in the cases of Y and Sc doping, In doping significantly increases the electrical conductivity and widens the optical band gap. In contrast, because of the small ionic radius of Ga, large structural relaxation reduces the Cd 5s–O 2p hybridization, and as a result, the optical band gap is increased only modestly. Experimentally, we find that In and Ga doping widens the band gap from 2.85 to 3.18 and 3.08 eV, respectively, via a Burstein–Moss (B–M) shift. Thin films with maximum conductivities of 10 400 and 20 000 S/cm on glass and MgO(100), respectively, are obtained at In doping levels of 4.3%. and 2.6%. The Ga doping, however, only increases the conductivity to 11 500 S/cm at 1.6% Ga doping on MgO (100) substrates, and the doping of Ga on glass substrates does not increase the conductivity significantly. Epitaxial films grown on MgO(100) also exhibit a biaxial, highly textured microstructure, leading to higher doping efficiency and fewer scattering centers, which is suggested to be responsible for the higher conductivity vs the films on glass.[25]

Our theoretical and experimental results reveal that dopant ion size and its electronic configuration have a significant influence on the CdO-based TCO crystal and band structures as well as on the optical and electrical properties. First, Ga^{3+} (0.76 Å), In^{3+} (0.94 Å), and Sc^{3+} (0.89 Å), with smaller ion sizes than that of Cd^{2+} (1.09 Å), compress the lattice parameters, while Y (1.04 Å), with an ion size similar to that of Cd^{2+}, does not significantly alter the lattice parameter. Ga (0.76 Å), with the smallest radius among the four dopants, only compresses the lattice slightly and exhibits low doping

efficiency. Second, in contrast to In-doped CdO, the large structural relaxation in CGO reduces the Cd 5s–O 2p hybridization, which in turn significantly affects the dispersion of the conduction band. The resulting small electron velocity along with the low doping efficiency of Ga explains the lower mobility in CGO as compared to In-doped CdO. The experimental observations agree well with the theoretical predictions.

On the basis of results of the present studies, it can be seen that CdO-based TCO films generally exhibit higher carrier mobilities than do those of In_2O_3-, ZnO-, and SnO_2-based TCO materials. This can be ascribed to the simple CdO cubic crystal structure, the broadly dispersed free-electron-like Cd 5s-based conduction band, and the low carrier effective masses. We find that dopant ion size has a substantial influence on the transport and optical properties of CdO, specifically, on the width of the highly dispersed conduction band and its location with respect to the band edges, which provide the necessary conditions for optimizing transparent conducting behavior with doping.

Acknowledgment. This work was supported by the NREL (XAF5-33636-02), the NSF-MRSEC program (Grant DMR-0520513) at the Northwestern Materials Research Center, and a computer time grant from the NSF at MCA96S016. We thank Dr. J. Carsello for his assistance with X-ray diffraction measurements.

CM702588M